Titanium-released from dental implant enhances pre-osteoblast adhesion by ROS modulating crucial intracellular pathways

Rossi MC; Bezerra FJB; Silva RA; Crulhas, BP; Fernandes CJC; Nascimento AS; Pedrosa VA; Padilha P; Zambuzzi WF[‡]

Dept. of Chemistry and Biochemistry, Bioscience Institute, State University of São Paulo – UNESP, *campus* Botucatu, Botucatu, São Paulo, Brazil.

[‡]Corresponding author:
Willian F. Zambuzzi, PhD
Head of Bioassays and Cellular Dynamic Lab,
Dept. of Chemistry and Biochemistry
Biosciences Institute / IBB-UNESP
P.O. Box: 510, Zip Code: 18618-970
Rubião Jr – Botucatu – São Paulo – Brazil
e-mail: wzambuzzi@ibb.unesp.br
Phone: +55 14 3880-0599

Abstract

It is important to understand the cellular and molecular events that occur at the cell–material interface of implants used for bone repair. The mechanisms involved in the initial stages of osteoblast interactions with the surface of the implant material must be decisive for cell fating surrounding them. In order to address this issue, we decided to investigate if conditioned medium for dental implants was able to modulate murine pre-osteoblast metabolism. First, we determined the concentration of titanium (Ti)-containing conditioned medium and found that it was 2-fold increased ($p<0.0001$). We have reported that this conditioned medium significantly up-modulated pre-osteoblast adhesion up to 24 hours ($p<0.0001$). In parallel, our results showed that both phosphorylations of FAK (Focal Adhesion Kinase) at Y397 ($p<0.0011$) and cofilin at Ser03 ($p<0.0053$) were also up-modulated, as well as for Rac1 expression ($p<0.0175$); both of them are involved with cell adaptation by rearranging cytoskeleton actin filaments. Thereafter, Ti-containing medium stimulated ROS (Reactive Oxygen Species) production by pre-osteoblast cells, and it is very possible that ROS compromised PTP-1B (Protein Tyrosine Phosphatase 1B) activation since PTP1B was down-phosphorylated ($p<0.0148$). The low PTP activity guarantees the phosphorylation of FAK at Y-residue, causing better pre-osteoblast adhesion in response to Ti-containing medium. Altogether, these data indicate that ROS indirectly modulate FAK phosphorylation in response to Ti-released from dental implants. Taken the results in account, these data showed for the first time that the implanted dental device is able to dynamically affect surrounding tissues, mainly by promoting a better performance of the pre-osteoblast cells.

Keywords: Dental Implants; Titanium; Pre-osteoblast; Signal transduction; Cell Adhesion.

1. INTRODUCTION

Titanium alloys are important materials used for dental devices, and their modification is a well-established strategy to strengthen their bioactivity while maintaining excellent biological properties [1-3]. The widespread application of titanium alloys in dental devices is clearly due to the combination of their mechanical performance with biological issues. In order to improve these alloys in biological systems, better implant materials are needed that present proper surface roughness to promote cell attachment [4,5]. The focus of biomaterials has shifted towards tissue engineering, complex medical applications, and biotechnology, therefore, there is a need to better define and evaluate the specific interaction between biomaterials and host's surrounding tissues.

Evaluation of the interaction between cells and implantable materials must consider parameters other than maintenance of cell viability and properly interfere on pre-osteoblast metabolism, activating adhesion molecules [4,6,7]. Over the last few years, we have addressed signal transduction mechanisms that govern the adhesion of osteoblasts on physico-chemically known surfaces so that they can serve as a parameter analysis for other tests, in which the cell attachment ability is unknown. Our recent study showed that, in the first 2 hours post-seeding, the metabolism of osteoblasts culminate in different signaling pathways responsible for cytoskeletal rearrangement [5,8-11]. Although some progress has been achieved on cell/biomaterial interaction [4,5,7,11-16], much remains to be understood, mainly regarding the indirect effect on the relationship of titanium alloys with the host tissue. In order to address this issue, we decided to elaborate a biological model by conditioning medium in contact with the dental implants for 24 hours, as recommended by ISO 10993-12 [17].

Proper cell contact with material surfaces and subsequent adhesion/spreading are the first stages in cell-material interactions [6,7]. These initial events profoundly influence the integration of dental implants into host tissue and determine the success or failure of a broad range of implanted biomaterials. The importance of these interactions has led to greater interest in understanding bone formation, particularly osteoblast adhesion and differentiation [18-20], as a means of predicting the quality of biological responses [9,12-14,18]. In order to address this very important issue in oral implantology, pre-osteoblasts were subjected to this conditioned medium and several approaches were applied to evaluate its effects on murine pre-osteoblast metabolism. More importantly, we demonstrated that ROS modulates FAK phosphorylation by an indirect way in response to Ti-released from dental implants. In addition, these data showed for the first time that the implanted dental device is able to dynamically affect surround tissues, mainly by promoting a better performance of pre-osteoblast cells.

2. Material and methods

2.1. Dental implant and reagents

The Strong SW dental conical implant was synthesized in titanium grade IV (Norm ASTM F67) and presented specific topography (Sa=0.99, S_q=1.21, Sd_r=80.1) as reported by Bonfante el al (2013) [29]; which were gently donated by the S.I.N. Co. (SP, BRAZIL).

The antibodies were purchased from Cell Signaling: β-Actin Antibody (#4967, 45kDa); Phospho-FAK (Tyr397) Antibody (#3283, 125kDa); Phospho-FAK (Tyr576/577) Antibody (#3281, 125kDa); Cofilin Antibody (#3312, 19kDa); Phospho-Cofilin (Ser3) (77G2) Rabbit mAb (#3313, 19kDa); Rac1/Cdc42 Antibody

(#4651, 21kDa); PTP1B Antibody (#5311, 50kDa), Anti-mouse, anti-rabbit, and

Abcam: Anti-FAK Antibody (ab61113, 119kDa); Anti-PTP1B (phospho S50)

Antibody (ab59419, 50kDa); Anti-PP2A alpha + beta Antibody [Y119] (ab32141,

35kDa); Anti-PP2A alpha + beta Antibody [E155] (ab32104, 35kDa).

2.2. Cell line and culture conditions

MC3T3-E1 (subclone 4), a preosteoblast cell line from mouse calvaria, was obtained

from American Type Culture Collection (Manassas, VA, USA) and grown at 37 °C in

α-MEM medium supplemented with 10% fetal bovine serum (FBS), 100 U/mL of

penicillin, and 100 g/mL of streptomycin under a humidified 5% CO_2 atmosphere. To

note, we have used cells ranging 10-15 passages and they are negative for

mycoplasma.

The implants (n = 6) were incubated in α-MEM medium for 24 h (ISO 10993:2016),

in order to establish the conditioned media. This conditioned media contains

molecules / particles potentially released by the implants. The conditioned media was

used to treat the cells in order to determine their viability, cell adhesion, and ability to

modulate the activation of intracellular proteins governing cell adhesion.

2.3. Cell viability assay

Samples were prepared according to ISO10993-12 (June 16, 2016), as used by

Zambuzzi et al. (2014) [17]. Briefly, the titanium dental implants were transferred to

conic tubes containing culture media (α-MEM) at a ratio of 0.2g/mL. After 24 h

incubation at 37 °C, extracts were collected and tested for viability, as follows. The

cells were then sub-cultured on 96-well plates at a cell density of 5 x 10^3 cells/mL.

After incubation for 24 h, the culture media was completely removed and substituted

by 180 µL/well of each sample extract (n=5) plus 20 µL 10% FBS. An internal

control was assayed by keeping the cells exposed solely to supplemented culture

medium. After 24 h exposure, the cell viability in response to each sample (extracts)

or controls were evaluated by a MTT reduction, MTT-test that measures

mitochondrial dehydrogenase activity by conversion of the yellow water-soluble

tetrazolium salt MTT into purple-colored soluble compound of formazan, by

measuring absorbance at 570 nm (Synergy II; BioTek Instruments, USA). Thus, the

production of formazan indirectly indicated cell viability.

2.4. Cell adhesion assay

To evaluate if the cells exhibited good adhesion in relation to the implant, the crystal

violet assay was done two different times. First, MC3T3-E1 cells were plated (50×10^3

cells) into two 24-wells and conditioned cultured in α-MEM with 10% of fetal bovine

serum (FBS) medium as mentioned earlier. After 24 h, both plates were treated with

conditioned media without SFB (half of each plate), and the two other halves were

treated with normal medium, also without serum. After 3 h, the absorbance was read

(microplate reader; Synergy II; BioTek Instruments, USA) at a wavelength of 590

nm. The second plate was read after 24 h.

2.5. Electrochemical detection of H_2O_2

A potentiostat µAutoLabIII (Metrohm, NL) was employed for all electrochemistry.

The electrochemical cell consisted of an Ag/AgCl (3 M KCl) reference electrode, a

platinum wire counter electrode placed, and Au working electrodes positioned inside

the electrochemical cell. Cyclic voltammetry (CV) was used to detect H_2O_2 released

by MC3T3-E1 cells. For electrochemistry measurements, 50×10^3 were incubated onto

the surface of the electrode. CV measurements were made every 20 min, during 2h,

and the calibration curve was constructed by plotting absolute value for reduction

current for anodic peak versus H_2O_2 concentration when compared to control (at the

beginning point of experiment). Limit of detection (LOD) was calculated based on

calibration curve using linear regression by the standard deviation of y-intercept

$(LOD = 3\sigma/Slope)$.

2.6. Scanning Electron Microscopy (S.E.M.)

Cells (50×10^3 cells) were plated onto the implant adhered in a well and incubated for

24 h. After this time, the implant was removed from the well and replaced in a 20mL

graduated glass Beaker containing 1.0 mL of 2.5% glutaraldehyde in 0.1 mol L^{-1}, pH

7.3 phosphate buffer maintained for 24 h in the refrigerator. Later, the implant was

taken a tube, pre-treated as necessary for the Electron Microscopy Center (IBB-

UNESP, Botucatu, Sao Paulo, Brazil). Finally, the implant was fitted and fixed in the

stub equipment scanning electron microscope (Quanta 200 - FEI Company), which

was metallized, and used energy of 12.5 Kv through a signal from the interaction of

electron beam to produce the images of interest.

2.7. Energy Dispersive Spectroscopy (EDX)

After S.E.M. analysis, we used an energy dispersive detector of x-ray contained in the

SEM to detect the existence of carbon and titanium elements in the sample. In

analyzing an electron beam focused on the mineral contained in the sample, the

outermost electrons of the atoms and the constituent ions were excited, changing

energy levels. To return to its initial position, they released the acquired energy that is

emitted at a wavelength in the X-ray spectrum. A detector installed in the vacuum chamber of the SEM measured the electron energy associated with this. Because the electrons of a given atom have different energies, it is possible to determine the chemical elements on site.

2.8. Quantification of titanium by graphite furnace atomic absorption spectrometry (GFAAS)

Initially, the implant-conditioned medium was used to measure titanium element content. To do so, 10 μL of each sample was removed for analysis of metalomic assay. The titanium determination was carried out by GFAAS using a SHIMADZU model AA-6800 atomic absorption spectrometer. This spectrometer was equipped with a background absorption corrector with a self-reverse system (SR), a pyrolytic graphite tube with an integrated platform and an ASC-6100 automatic sampler. A Shimadzu hollow cathode titanium lamp was used and operated at a minimum current of 12 mA and a maximum current of 400 mA (current used in background correction – BG). The wavelength was 364.3 nm, and the spectral resolution was 0.5 nm. Argon was used as the inert gas, and a constant flow of 1 L min^{-1} was maintained during the entire heating program except for the atomization stage, during which the gas flow was stopped. The absorbance measurements (based on the peak area) were carried out in triplicate. The graphite tube's heating program optimized for titanium determinations was based on the procedure described by Silva et al. (2006) [21] for chromium determination with some modification and it is described in following: Drying temperature – 120/250°C; Pyrolysis temperature – 900/1400°C; Atomization temperature – 2600°C and Cleanup temperature – 2800°C [21].

2.9. Immunoblotting

Cells were cultured on different surfaces. After 3 h, they were lysed and protein extracts were obtained using a Lysis Cocktail (50 mM Tris [tris(hydroxymethyl)aminomethane]–HCl [pH 7.4], 1% Tween 20, 0.25% sodium deoxycholate, 150 mM NaCl, 1 mM EGTA (ethylene glycol tetraacetic acid), 1 mM O-Vanadate, 1 mM NaF, and protease inhibitors [1 μg/mL aprotinin, 10 μg/mL leupeptin, and 1 mM 4-(2-amino-ethyl)-benzolsulfonyl-fluorid-hydrochloride]) for 2 h on ice. After sample's clearing by centrifugation, the protein concentration was determined using Lowry method. An equal volume of 2x sodium dodecyl sulfate (SDS) gel loading buffer (100 mM Tris-HCl [pH 6.8], 200 mM dithiothreitol [DTT], 4% SDS, 0.1% bromophenol blue, and 20% glycerol) was added to samples and boiled for 5 min. After, protein extracts were resolved by SDS-PAGE (10 or 12%) and transferred to PVDF membranes (Bio-Rad, Hercules, CA, USA). Membranes were blocked with either 1% fat-free dried milk or bovine serum albumin (2.5%) in Tris-buffered saline (TBS)–Tween 20 (0.05%) and incubated overnight at 4 °C with appropriate primary antibody at 1:1000 dilutions. After washing in TBS-Tween 20 (0.05%), membranes were incubated with horseradish peroxidase-conjugated anti-rabbit, anti-goat, or anti-mouse IgGs antibodies, at 1:2000 dilutions (in all immunoblotting assays), in blocking buffer for 1 h. Then, the detection was performed using enhanced chemiluminescence (ECL).

2.10. Confocal microscopy

MC3T3-E1 cells were seeded onto glass coverslips and incubated for 24 h at 37 °C in a humidified atmosphere containing 5% CO_2. Afterwards, the culture medium was replaced by titanium-conditioned medium and incubated for additional 24 h. One hour

before the end of treatment, 1 µM DCFDA or C11-BODIPY 581/591 was added to cell cultures. After washing in PBS, the glass coverslips containing pre-osteoblasts were mounted in Fluor-shield with DAPI (Sigma; USA). Cells were then analyzed using inverted laser scanning confocal microscope (Leica TCS SP5). The H2DCFDA was excited with a 488 nm argon laser and emission was detected by means of a bypass filter at 500–550 nm. For lipoperoxidation analysis, BODIPYC11 was excited with 488 nm laser and emission was detected via by pass at 495 to 540 for the oxidized form and 550–610 for the non-oxidized form of the BODIPY molecule and DAPI excited with 405 nm laser. For the oxidative stress and lipid peroxidation analysis, the treated group was excited with the same laser intensity as the control group. Adobe Photoshop 9.2 software was used for image preparation.

2.11. Statistics

Results were represented as mean ± standard deviation (SD). The samples assumed a normal distribution and they were subjected to student's t-test (2-tailed) with $p < 0.05$ considered statistically significant and $p < 0.001$ considered highly significant. In the experiment where there were > 2 groups, we used one-way ANOVA with post-test of Bonferroni, in order to compare all pairs of groups. In this case, the significance level was considered when alpha=0.05 (95% confidence interval). The software used was GraphPad Prism 6.

3. Results

3.1. Dental implant releases titanium at nanomolar concentration and does not

promote cytotoxicity

First, we prepared the conditioned medium by incubating the dental implants in conic

tubes at 37°C as recommended by ISO 10993-12:2016 up to 24 h. Thereafter, we used

this conditioned medium for treating the pre-osteoblasts and analyzing cell

metabolism. Thus, before treating the cells, we evaluated the content of titanium

released from dental implants and present at conditioned medium. Our result showed

that the dental implant interacts with the surrounding solution by significantly

releasing titanium elements ($p<0.0001$), as showed the **Fig.1a**. Then, we used this

conditioned medium to treat semiconfluent MC3T3-E1 pre-osteoblast cells in order to

check viable cells and it was not cytotoxicity (**Fig.1b**).

A chemical explanation for detecting an increase of the Ti in the medium needs

considering the pH of the medium buffered close to neutrality (pH = 7.30). As

titanium dioxide (TiO_2) layer formed on the surface of the implant at pH close to

neutrality can undergo very low hydrolysis, it is possible considerate the low releasing

traces of titanyl ions (TiO^{2+}).

3.2. Ti released from dental implants enhances pre-osteoblast adhesion by up-

modulating FAK (Y397) and Cofilin (Ser03) phosphorylations

Because conditioned medium did not present cytotoxicity, we decided to evaluate its

influence on pre-osteoblast adhesion. Thus, we treated semiconfluent cell cultures up

to 24 h, when they were trypsinized, counted, and re-seeded in 96-well culture plates.

Curiously, our result showed that conditioned medium affected cell metabolism, significantly up-modulating cell adhesion up to 24 h from seeding. We were encouraged to understand the modulation of specific protein activation in this scenario, and we found that the cells treated with conditioned medium showed a significant up-modulation of FAK phosphorylation (Y397, **Fig.1e**, p<0.0011), as well as rac-1 expression (**Fig.1f**, p<0.0175) for those cells. In addition, we assayed the phosphorylation of cofilin in this context, and there was also an up-phosphorylation (**Fig.1g**, p<0.0053) in response to Ti released from dental implants containing conditioned medium. The **Fig.1d** presents representative western blot images.

Moreover, because the conditioned medium is able to modulate crucial signaling protein involved with cell adhesion, such as FAK and Cofilin, we seeded pre-osteoblast on dental implant in order to evaluate cell morphological behavior. The osteoblast seemed to interact well with the surface of dental implants, because cell spreading and cytoplasmic elongation were identified (**Figs.2a-c**). Later, by using EDX approach, it was possible to identify carbon (**Fig.2e**) and titanium (**Fig.2f**) elements on the surface.

3.3. Ti released from dental implants cause an increase of ROS production in pre-osteoblast culminating on PTP-1B down-phosphorylation and increased lipid peroxidation

For the electrochemical detection of H_2O_2, the cells (50×10^3 cells) were plated in petri dishes and treated with the conditioned medium (exactly as detailed elsewhere). Here, we considered the cells subjected to a normal α-MEM as a control group. Thus, both

groups (control and treated with conditioned medium) were incubated for 24 h under the same environment conditions, when the cells were trypsinized and immediately followed for an electroanalytical detection of H_2O_2 (ROS). To note, MC3T3-E1 cells did not attach on top of electrodes due to non-fouling properties of PEG. Measurements were made every 20 min during 2 h. The electrochemical biosensor was used for H_2O_2 monitoring due to possibility for *in situ* measurements and real time detection (**Fig.3a**), providing reliable results without requiring multiple-step experiments. Release of H_2O_2 was detected with CV by diffusion of H_2O_2 inside hydrogel. H_2O_2 is an electroactive compound that was verified in the reduction process in absence and presence of AuNPs-conjugated horseradish peroxidase (HRP) and PEG Hydrogel. For control experiments, CV did not showed a representatives cathodic and anodic peak, and after 2 h of measurement only a small reduction was achieved in current for anodic peak, which demonstrates a minimal amount of H_2O_2 released by cells. For the dental implant group, incorporation of hydrogen peroxide inside the hydrogel matrix was detected, and increased current response in both positive and negative potential was achieved (**Fig.3b**). Increased reduction current for H_2O_2 monitoring was observed right after the first measurement, which indicates constant production of H_2O_2 from MC3T3-E1 cells (**Fig.3c**). Reduction current did not saturate after 2 h, proving the feasibility and stability of the sensor, which was not compromised by non-specific proteins and byproduct released by MC3T3-E1 cells.

In addition, these cells were seeded on glass coverslips and again subjected to Ti-containing medium. Later these cells were incubated with DCFDA or BODIPY C11 probes, to identify ROS content and Lipid peroxidation respectively. Thus, we identified an increase of the ROS in pre-osteoblast cells in response to Ti-containing

medium from dental implants (**Fig.4**). Curiously, pre-osteoblast in response to Ti-containing medium had increased lipid peroxidation (**Fig.5**), but without triggering cell death signaling.

At the same time, phophorylation of PTP-1B was also investigated in order to check its involvement with the maintenance of FAK phosphorylation because PTP-1B can dephosphorylate FAK. Immunoblottings showed that PTP-1B phosphorylation was down-regulated (**Fig.6**) in response to Ti-containing medium from dental implants.

Finally, **Fig.7** presents a general mechanism obtained in this work, illustrating that ROS released in response to Ti-containing medium modulates FAK phosphorylation by down-regulating PTP-1B activity; here shown by evaluating phosphorylation of PTP-1B.

4. Discussion

We have shown for the first time that dental implants modulate surrounding tissue by releasing soluble Titanium (Ti) and enhancing pre-osteoblast performance by up-stimulating FAK phosphorylation at Y397 residue and cofilin at S03 residue. FAK is an important transducer involved in signal transduction pathway after integrin activation and plays a role in guiding cell adhesion and migration. When stimulated by integrin activation, FAK autophosphorylates at Y397 exposing specific domains for interacting with Src [5,10,22]. Previously, we have proposed both FAK and Src as critical bio-parameters to predict the quality of pre-osteoblast adhesion [7,9,18,23]. Thus, because dental implants evaluated in this study are able to release Ti elements and later control cell adhesion, this mechanism is probably responsible for self-

renewing osteoblast cells during cell-coupled bone remodeling, which guarantees the quality of bone in contact with the implants.

In addition, this work also showed that conditioned medium from dental implants modulates ROS production in treated pre-osteoblast cells. This is a very relevant topic to be considered because ROS are well-known physiological inhibitors of Protein Tyrosine Phosphatases (PTPs); PTPs regulate signal transduction pathways and they are regulated by a reversible oxidization of the catalytic cysteine to sulphenic acid (Cys-SOH) [24,25]. In this way, in order to comprehend the activation of PTPs, we investigated PTP-1B since its widely involved in cellular mechanism including FAK phosphorylation control [25,26]. In fact, our results support the hypothesis that ROS negatively modulate PTP activity, resulting in more general and expressive Y-phosphorylation balance, because PTPs dephosphorylate Y-residues in cell metabolism [24,25], mainly affecting FAK, a PTK involved with signal transduction governing cell adhesion. In this case, PTP-1B activity was proposed by evaluating its pattern of phosphorylation.

Finally, confocal microscopy approaches also show that ROS production in response to conditioned medium promoted lipid peroxidation (LP). LP is a biochemical process under which free radicals attack lipids containing carbon-carbon double bond, especially polyunsaturated fatty acids that involve hydrogen abstraction from a carbon, with oxygen insertion resulting in lipid peroxyl radicals and hydroperoxides [27]. In general, LP has been related with cell apoptosis; however, Fuhrman, Oiknine & Aviram (1994) [28] showed that LP has interesting parameters during metallic metabolism without cell death, as we found for titanium released from dental implants. Those authors demonstrated for the first time that iron ions could induce lipid peroxidation in intact macrophages without causing cell death at 50 μM of

$FeSO_4$ for 4 h at 37 °C. From our experiment, it is very hard to estimate the amount of ROS or LP, but we showed that 1 ng/mL of tytanil ions generates enough oxidative stress which governs indirectly FAK activation and mediates cell adhesion by consequently promoting cytoskeleton rearrangement identified here by the phosphorylation of cofilin.

5. Conclusion

Up until now, the influence of Ti-released from dental implants on pre-osteoblast performance has not been studied. This study investigated the hypothesis that conditioned medium from dental implants modulates pre-osteoblast performance by governing crucial intracellular pathways. Our results showed that Ti-released from dental implants enhanced pre-osteoblast adhesion by oxidative stress modulating phosphorylation balance of crucial signaling proteins such as FAK and PTP-1B. This suggests that dental implants promote a very dynamic relationship with surrounding tissues in an intense remodeling manner.

References

1. Anitua E, Piñas L, Murias A, Prado R, Tejero R. Effects of calcium ions on titanium surfaces for bone regeneration. Colloids Surf B Biointerfaces. 2015 Jun 1;130:173-81.
2. Fraioli R, Rechenmacher F, Neubauer S, Manero JM, Gil J, Kessler H, Mas-Moruno C. Mimicking bone extracellular matrix: integrin-binding peptidomimetics enhance osteoblast-like cells adhesion, proliferation, and differentiation on titanium. Colloids Surf B Biointerfaces. 2015 Apr 1;128:191-200.
3. Jenny G, Jauernik J, Bierbaum S, Bigler M, Grätz KW, Rücker M, Stadlinger B. A systematic review and meta-analysis on the influence of biological implant surface coatings on periimplant bone formation. J Biomed Mater Res A. 2016 Nov;104(11):2898-910.
4. Zambuzzi WF, Coelho PG, Alves GG, Granjeiro JM. Intracellular signal transduction as a factor in the development of "smart" biomaterials for bone tissue engineering. Biotechnol Bioeng. 2011 Jun;108(6):1246-50.
5. Gemini-Piperni S, Milani R, Bertazzo S, Peppelenbosch M, Takamori ER, Granjeiro JM, Ferreira CV, Teti A, Zambuzzi W. Kinome profiling of osteoblasts on hydroxyapatite opens new avenues on biomaterial cell signaling. Biotechnol Bioeng. 2014 Sep;111(9):1900-5.
6. Anselme K. Osteoblast adhesion on biomaterials. Biomaterials. 2000 Apr;21(7):667-81
7. Zambuzzi WF, Ferreira CV, Granjeiro JM, Aoyama H. Biological behavior of pre-osteoblasts on natural hydroxyapatite: a study of signaling molecules from attachment to differentiation. J Biomed Mater Res A. 2011 May;97(2):193-200.
8. Zambuzzi WF, Bruni-Cardoso A, Granjeiro JM, Peppelenbosch MP, de Carvalho HF, Aoyama H, Ferreira CV. On the road to understanding of the osteoblast adhesion: cytoskeleton organization is rearranged by distinct signaling pathways. J Cell Biochem. 2009 Sep 1;108(1):134-44.
9. Milani R, Ferreira CV, Granjeiro JM, Paredes-Gamero EJ, Silva RA, Justo GZ, Nader HB, Galembeck E, Peppelenbosch MP, Aoyama H, Zambuzzi WF. Phosphoproteome reveals an atlas of protein signaling networks during osteoblast adhesion. J Cell Biochem. 2010 Apr 1;109(5):957-66.
10. Zambuzzi WF, Milani R, Teti A. Expanding the role of Src and protein-tyrosine phosphatases balance in modulating osteoblast metabolism: lessons from mice. Biochimie. 2010 Apr;92(4):327-32.
11. Gemini-Piperni S, Takamori ER, Sartoretto SC, Paiva KB, Granjeiro JM, de Oliveira RC, Zambuzzi WF. Cellular behavior as a dynamic field for exploring bone bioengineering: a closer look at cell-biomaterial interface. Arch Biochem Biophys. 2014 Nov 1;561:88-98.
12. Bertazzo S, Zambuzzi WF, da Silva HA, Ferreira CV, Bertran CA. Bioactivation of alumina by surface modification: a possibility for improving the applicability

of alumina in bone and oral repair. Clin Oral Implants Res. 2009 Mar;20(3):288-93.

13. Bertazzo S, Zambuzzi WF, Campos DD, Ferreira CV, Bertran CA. A simple method for enhancing cell adhesion to hydroxyapatite surface. Clin Oral Implants Res. 2010 Dec;21(12):1411-3.

14. Bertazzo S, Zambuzzi WF, Campos DD, Ogeda TL, Ferreira CV, Bertran CA. Hydroxyapatite surface solubility and effect on cell adhesion. Colloids Surf B Biointerfaces. 2010 Jul 1;78(2):177-84.

15. Castro-Silva II, Zambuzzi WF, de Oliveira Castro L, Granjeiro JM. Periosteal-derived cells for bone bioengineering: a promising candidate. Clin Oral Implants Res. 2012 Oct;23(10):1238-42.

16. Zambuzzi WF, Oliveira RC, Subitoni BL, Menezes R, Taga R, Granjeiro JM. Biological monitoring of a promissory xenogenic pin for biomedical applications: a preliminary intraosseous study in rats. Clin Oral Implants Res. 2012 Mar;23(3):367-72.

17. Zambuzzi WF, Bonfante EA, Jimbo R, Hayashi M, Andersson M, Alves G, Takamori ER, Beltrão PJ, Coelho PG, Granjeiro JM. Nanometer scale titanium surface texturing are detected by signaling pathways involving transient FAK and Src activations. PLoS One. 2014 Jul 7;9(7):e95662.

18. Zambuzzi WF, Granjeiro JM, Parikh K, Yuvaraj S, Peppelenbosch MP, Ferreira CV. Modulation of Src activity by low molecular weight protein tyrosine phosphatase during osteoblast differentiation. Cell Physiol Biochem. 2008;22(5-6):497-506.

19. Zambuzzi WF, Paiva KB, Menezes R, Oliveira RC, Taga R, Granjeiro JM. MMP-9 and CD68(+) cells are required for tissue remodeling in response to natural hydroxyapatite. J Mol Histol. 2009 Aug;40(4):301-9.

20. de Souza Malaspina TS, Zambuzzi WF, dos Santos CX, Campanelli AP, Laurindo FR, Sogayar MC, Granjeiro JM. A possible mechanism of low molecular weight protein tyrosine phosphatase (LMW-PTP) activity modulation by glutathione action during human osteoblast differentiation. Arch Oral Biol. 2009 Jul;54(7):642-50.

21. Silva FA, Padilha CCF, Pezzato LE, Barros MM, Padilha PM. Determination of chromium by GFAAS in slurries of fish feces to estimate the apparent digestibility of nutrients in feed used in pisciculture. Talanta 2006 June: 69(4): 1025-1030.

22. Mitra SK, Hanson DA, Schlaepfer DD. Focal adhesion kinase: in command and control of cell motility. Nat Rev Mol Cell Biol. 2005 Jan;6(1):56-68.

23. Zambuzzi WF, Yano CL, Cavagis AD, Peppelenbosch MP, Granjeiro JM, Ferreira CV. Ascorbate-induced osteoblast differentiation recruits distinct MMP-inhibitors: RECK and TIMP-2. Mol Cell Biochem. 2009 Feb;322(1-2):143-50.

24. Ferreira CV, Justo GZ, Souza AC, Queiroz KC, Zambuzzi WF, Aoyama H, Peppelenbosch MP. Natural compounds as a source of protein tyrosine phosphatase inhibitors: application to the rational design of small-molecule derivatives. Biochimie. 2006 Dec;88(12):1859-73.

25. Fernandes GV, Cavagis AD, Ferreira CV, Olej B, Leão Mde S, Yano CL, Peppelenbosch M, Granjeiro JM, Zambuzzi WF. Osteoblast adhesion dynamics: a possible role for ROS and LMW-PTP. J Cell Biochem. 2014 Jun;115(6):1063-9.

26. Arregui CO, González Á, Burdisso JE, González Wusener AE. Protein tyrosine phosphatase PTP1B in cell adhesion and migration. Cell Adh Migr. 2013 Sep-Oct;7(5):418-23.

27. Ayala A, Muñoz MF, Argüelles S. Lipid peroxidation: production, metabolism, and signaling mechanisms of malondialdehyde and 4-hydroxy-2-nonenal. Oxid Med Cell Longev. 2014;2014:360438.

28. Fuhrman B, Oiknine J, Aviram M. Iron induces lipid peroxidation in cultured macrophages, increases their ability to oxidatively modify LDL, and affects their secretory properties. Atherosclerosis. 1994 Nov;111(1):65-78.

29. Bonfante EA, Granato R, Marin C, Jimbo R, Giro G, Suzuki M, Coelho PG. Biomechanical testing of microblasted, acid-etched/microblasted, anodized, and discrete crystalline deposition surfaces: an experimental study in beagle dogs. Int J Oral Maxillofac Implants. 2013 Jan-Feb;28(1):136-42.

30. FIGURE CAPTIONS

Fig. 1. Conditioned medium properties and its influence on osteoblast adhesion.

a. Dental implants release Ti to medium. The culture medium used in our experimental model was used for conditioning dental implants for 24 h, as previously detailed. Afterwards, the conditioned medium was taken for quantification of Ti element. Our results showed a significant increase in the Ti concentration when considering its immediate control group, where the culture medium was tested without conditioning with dental implants. *means statistical difference ($p < 0.0001$), when applied to the non-parametric t-test; **b.** Conditioned medium by dental implants does not promote cytotoxicity. Osteoblasts were treated for 24 h with conditioned medium from commercial implants. To evaluate the cell viability after treatment, the cells were incubated for 3 h with culture medium containing MTT salt (1 mg/ml). Next, the culture medium was completely aspirated and the blue formazam formed was dissolved in absolute ethanol and the absorbance measured at 550 nm; **c.** Ti released by dental implant significantly affected the adhesion of pre-osteoblasts. Cell adhesion evaluation was verified by colorimetric Crystal Violet test. The test was performed 3 h and 24 h after re-plating treatment. The control group (CTRL) was considered the culture medium without conditioning with the dental implant. *means statistical difference ($p < 0.0001$); **d**. Representative blotting of pFAK (Y397), Rac-1, Cofilin, pCofilin (Ser03), and β-Actin. Graphs **e** and **f** show arbitrary values obtained from densitometric analysis of pFAK (Y397) and Rac-1 bands normalized by the average values of the respective ß-Actin arbitrary values. The proteins pFAK (Y397) ($p = 0.0011$) and Rac-1 ($p = 0.0175$) were differentially expressed between the two treatment studied. Graph **g** gives arbitrary values obtained by densitometric analysis of pCofilin (Ser03) bands normalized by the average values of the respective Cofilin values. pCofilin (Ser03) ($p < 0.0001$) were differentially expressed between the two treatments studied. ß-Actin was used as loading sample (approximately 75 µg of protein per lane). *means statistical difference (test t-student).

Fig.2. Pre-osteoblast morphological changes when in interacting on dental implant surfaces. Pre-osteoblasts were seeded on dental implants (roughness related properties: $S_a = 0.99$, $S_q = 1.21$, $S_r = 80.1$), and after 24 h, they were processed by electron microscopy. **a.** Electron micrograph of dental implant surface; The electron micrographs showed that pre-osteoblast likely spread on the surfaces by interacting on

the mechanically produced roughness surfaces (**b-c**). EDX-based electron micrographs identifying Carbon (**e**) and Titanium (**f**) on the dental surfaces used in this work.

Fig.3. Electrochemical detection of H_2O_2 in response to dental implants in conditioned medium. First, cyclic voltammetry (CV) was used to detect H_2O_2 produced by MC3T3-E1 cells. CV measurements were made every 20 min during 2h, and calibration curve was constructed by plotting absolute value for reduction current for anodic peak versus H_2O_2 concentration when compared to control (beginning of experiment). The electrochemical cell consisted of an Ag/AgCl (3 M KCl) reference electrode, a platinum wire counter electrode placed, and Au working electrodes positioned inside the electrochemical cell. **a.** Plot showing absolute value of the reduction current as a function of H_2O_2 released by cells on control group (•) and dental implant group (▪). **b.** Cyclic voltammograms of HRP-AuNP-PEG Au electrode on control group without dental implant. **c.** Cyclic voltammograms of HRP-AuNP-PEG Au electrode on dental implant group. Measurements were made every 20 min.

Fig. 4. Effects of Titanium-conditioned medium on intracellular ROS production. MC3T3-E1 cells were seeded onto sterile coverslips and after 24 h were challenged with Titanium-conditioned medium for 24 h. Intracellular ROS production was detected by confocal microscopy after incubation of the cells with oxidative-sensitive fluorescent probe DCFH. The nuclei were stained with DAPI (blue). Bar = 50μm. Images represent two independent experiments.

Fig.5. ROS modulating intracellular pathways provoke PTP-1B down-phosphorylation. Dental implants release Ti to medium. The culture medium in our experimental model was used to condition dental implants for 24 h, as previously detailed. The cells were cultured under routine classic conditions, and in the semi-confluence, they were subjected to conditioned medium and after 24 h were lysed using standard lysing buffer (described in M&M). The protein pool was resolved on SDS-PAGE gel and then transferred to PVDF membrane. Signaling proteins were identified specifically by using specific primary antibody in Western blotting protocol. **a.** Representative blotting of PTP-1B and pPTP-1B; **b.** graph represents arbitrary values obtained from densitometry analysis and causes pPTP-1B/PTP-1B.

Our analysis found significance between control and Ti-treated pre-osteoblast cells (p=0.0148). ß-Actin was used as loading sample (approximately 75 μg of protein per race). *means statistical difference (test *t*-student).

Fig. 6. Effects of titanium-conditioned medium on lipid peroxidation. MC3T3-E1 cells were seeded onto sterile coverslips and after 24 h were challenged with Titanium-conditioned medium for 24 h. Lipid peroxidation was detected by confocal microscopy after incubation of the cells with C11-BODIPY581/591 probe excited with 488 nm laser and monitored simultaneously at 510 nm and 610 nm. Fluorescence micrographs obtained by confocal microscopy analysis revealed increased green fluorescence intensity (oxidized probe). The nuclei were stained with DAPI (blue). Bar = 50μm. Images represent two independent experiments.

Fig. 7. Signal transduction mechanisms involved in the response to released titanium. Schematic proposal cell signaling pathway where released titanium promoted an increase of ROS production, which is responsible to negatively control PTP-1B activity. In turn, PTP-1B modulated FAK phosphorylation, culminating on cytoskeleton rearrangement and later pre-osteoblast adhesion.
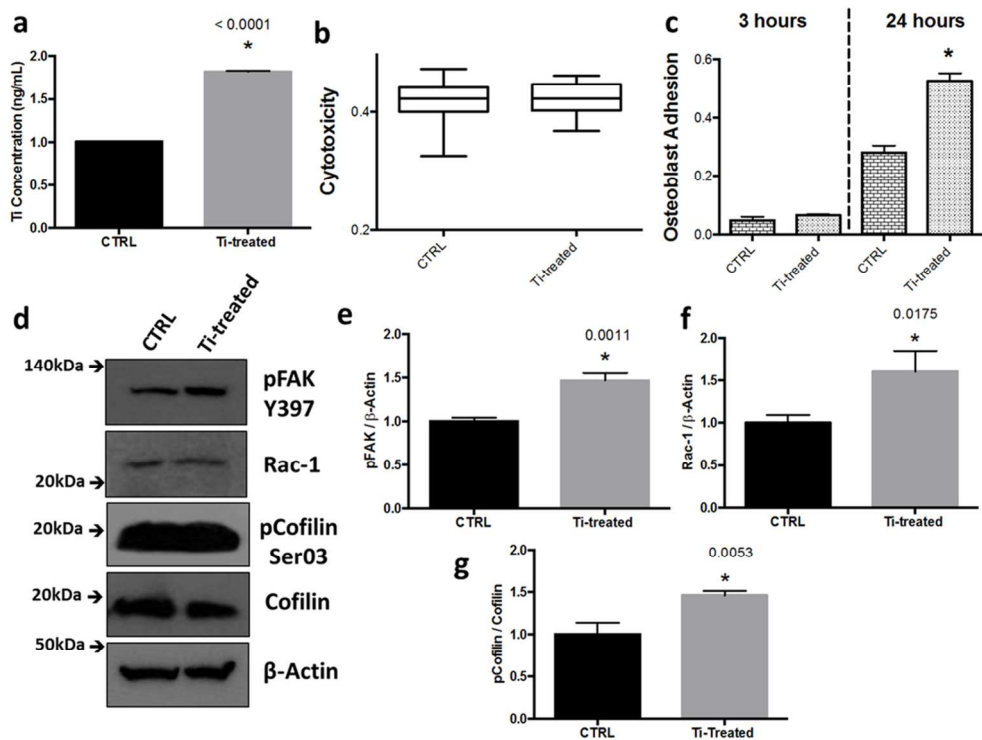
22

Fig. 1. Conditioned medium properties and its influence on osteoblast adhesion. a. Dental implants release Ti to medium. The culture medium used in our experimental model was used for conditioning dental implants for 24 h, as previously detailed. Afterwards, the conditioned medium was taken for quantification of Ti element. Our results showed a significant increase in the Ti concentration when considering its immediate control group, where the culture medium was tested without conditioning with dental implants. *means statistical difference (p<0.0001), when applied to the non-parametric t-test; b. Conditioned medium by dental implants does not promote cytotoxicity. Osteoblasts were treated for 24 h with conditioned medium from commercial implants. To evaluate the cell viability after treatment, the cells were incubated for 3 h with culture medium containing MTT salt (1 mg/ml). Next, the culture medium was completely aspirated and the blue formazam formed was dissolved in absolute ethanol and the absorbance measured at 550 nm; c. Ti released by dental implant significantly affected the adhesion of pre-osteoblasts. Cell adhesion evaluation was verified by colorimetric Crystal Violet test. The test was performed 3 h and 24 h after re-plating treatment. The control group (CTRL) was considered the culture medium without conditioning with the dental implant. *means statistical difference (p<0.0001); d. Representative blotting of pFAK (Y397), Rac-1, Cofilin, pCofilin (Ser03), and β-Actin. Graphs e and f show arbitrary values obtained from densitometric analysis of pFAK (Y397) and Rac-1 bands normalized by the average values of the respective ß-Actin arbitrary values. The proteins pFAK (Y397) (p=0.0011) and Rac-1 (p=0.0175) were differentially expressed between the two treatment studied. Graph g gives arbitrary values obtained by densitometric analysis of pCofilin (Ser03) bands normalized by the average values of the respective Cofilin values. pCofilin (Ser03) (p<0.0001) were differentially expressed between the two treatments studied. ß-Actin was used as loading sample (approximately 75 µg of protein per lane). *means statistical difference (test t-student).
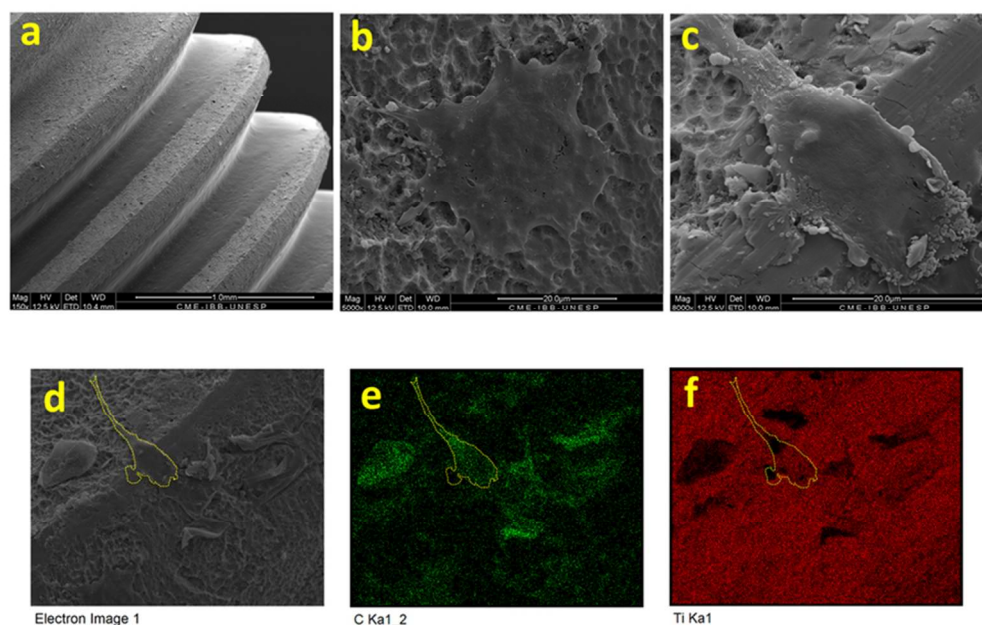
48x36mm (600 x 600 DPI)

Fig.2. Pre-osteoblast morphological changes when in interacting on dental implant surfaces. Pre-osteoblasts were seeded on dental implants (roughness related properties: Sa=0.99, Sq=1.21, Sdr=80.1), and after 24 h, they were processed by electron microscopy. a. Electron micrograph of dental implant surface; The electron micrographs showed that pre-osteoblast likely spread on the surfaces by interacting on the mechanically produced roughness surfaces (b-c). EDX-based electron micrographs identifying Carbon (e) and Titanium (f) on the dental surfaces used in this work.

38x24mm (600 x 600 DPI)

Fig.3. Electrochemical detection of H2O2 in response to dental implants in conditioned medium. First, cyclic voltammetry (CV) was used to detect H2O2 produced by MC3T3-E1 cells. CV measurements were made every 20 min during 2h, and calibration curve was constructed by plotting absolute value for reduction current for anodic peak versus H2O2 concentration when compared to control (beginning of experiment). The electrochemical cell consisted of an Ag/AgCl (3 M KCl) reference electrode, a platinum wire counter electrode placed, and Au working electrodes positioned inside the electrochemical cell. a. Plot showing absolute value of the reduction current as a function of H2O2 released by cells on control group (•) and dental implant group (·). b. Cyclic voltammograms of HRP-AuNP-PEG Au electrode on control group without dental implant. c. Cyclic voltammograms of HRP-AuNP-PEG Au electrode on dental implant group. Measurements were made every 20 min.
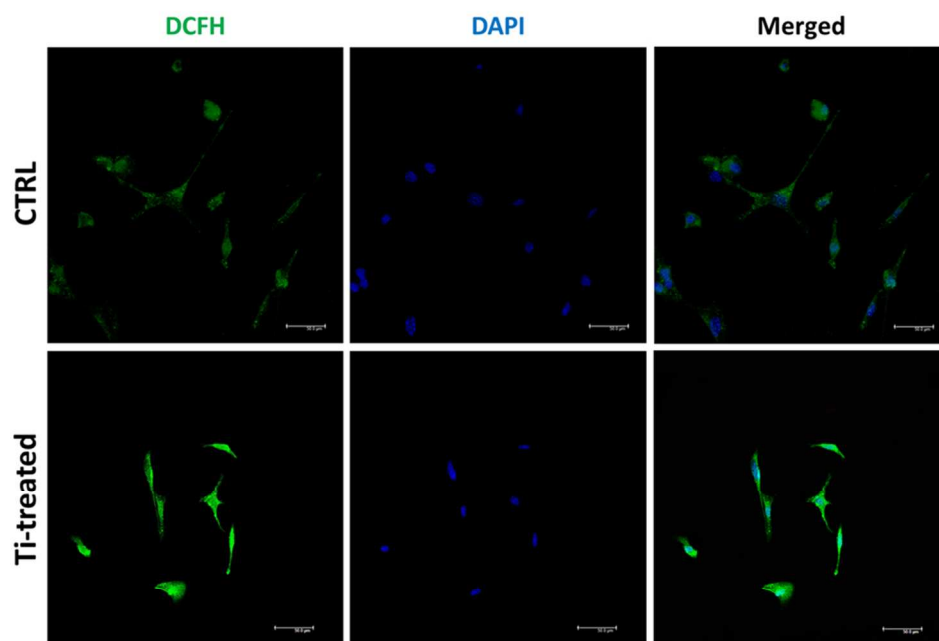
154x113mm (300 x 300 DPI)

Fig. 4. Effects of Titanium-conditioned medium on intracellular ROS production. MC3T3-E1 cells were seeded onto sterile coverslips and after 24 h were challenged with Titanium-conditioned medium for 24 h. Intracellular ROS production was detected by confocal microscopy after incubation of the cells with oxidative-sensitive fluorescent probe DCFH. The nuclei were stained with DAPI (blue). Bar = 50μm. Images represent two independent experiments.
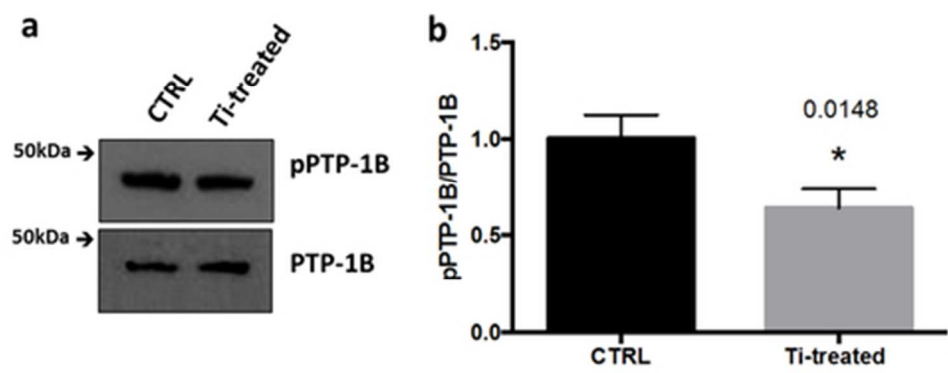
44x30mm (600 x 600 DPI)

Fig.5. ROS modulating intracellular pathways provoke PTP-1B down-phosphorylation. Dental implants release Ti to medium. The culture medium in our experimental model was used to condition dental implants for 24 h, as previously detailed. The cells were cultured under routine classic conditions, and in the semi-confluence, they were subjected to conditioned medium and after 24 h were lysed using standard lysing buffer (described in M&M). The protein pool was resolved on SDS-PAGE gel and then transferred to PVDF membrane. Signaling proteins were identified specifically by using specific primary antibody in Western blotting protocol. a. Representative blotting of PTP-1B and pPTP-1B; b. graph represents arbitrary values obtained from densitometry analysis and causes pPTP-1B/PTP-1B. Our analysis found significance between control and Ti-treated pre-osteoblast cells (p=0.0148). ß-Actin was used as loading sample (approximately 75 µg of protein per race). *means statistical difference (test t-student).
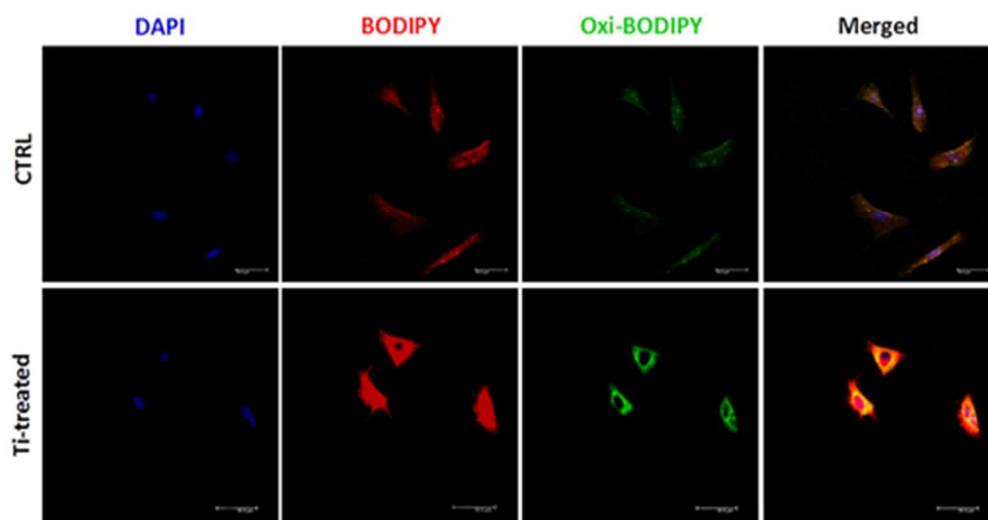
21x8mm (600 x 600 DPI)

Fig. 6. Effects of titanium-conditioned medium on lipid peroxidation. MC3T3-E1 cells were seeded onto sterile coverslips and after 24 h were challenged with Titanium-conditioned medium for 24 h. Lipid peroxidation was detected by confocal microscopy after incubation of the cells with C11-BODIPY581/591 probe excited with 488 nm laser and monitored simultaneously at 510 nm and 610 nm. Fluorescence micrographs obtained by confocal microscopy analysis revealed increased green fluorescence intensity (oxidized probe). The nuclei were stained with DAPI (blue). Bar = 50µm. Images represent two independent experiments.
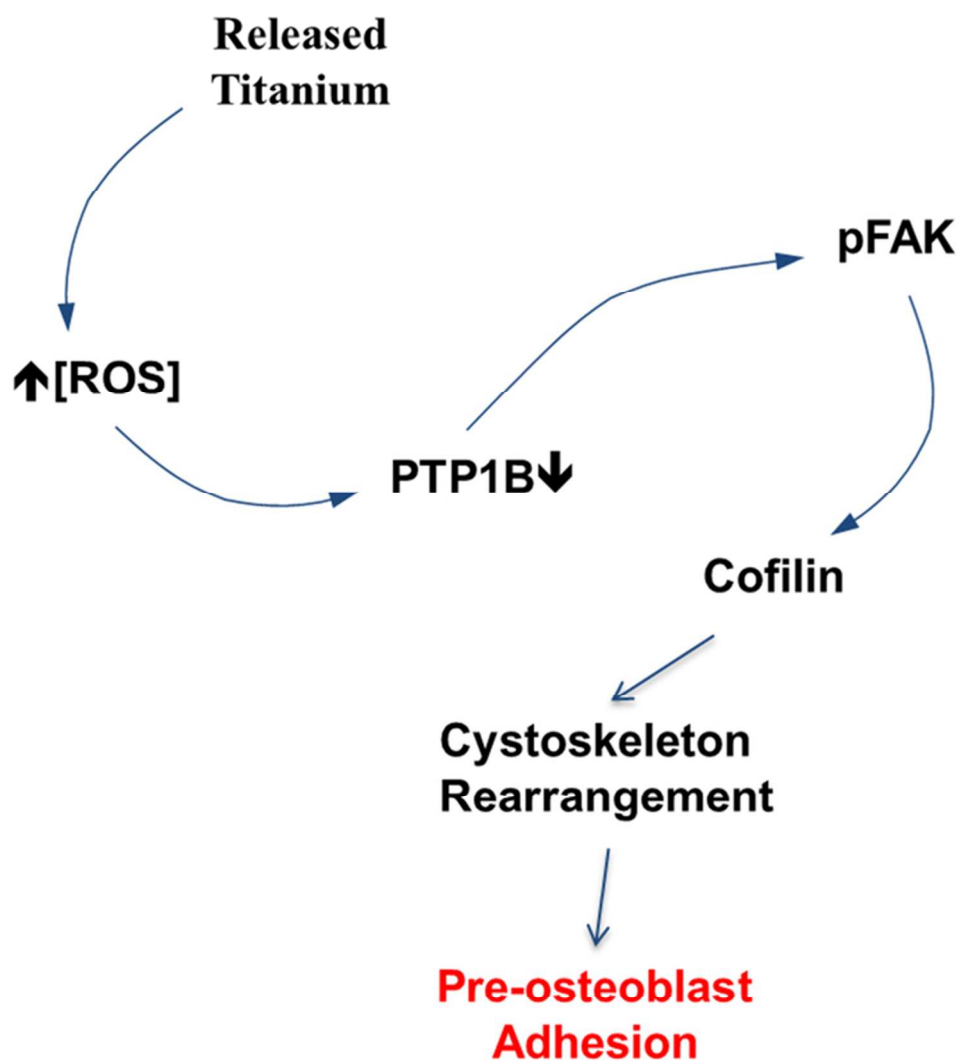
22x11mm (600 x 600 DPI)

Fig. 7. Signal transduction mechanisms involved in the response to released titanium. Schematic proposal cell signaling pathway where released titanium promoted an increase of ROS production, which is responsible to negatively control PTP-1B activity. In turn, PTP-1B modulated FAK phosphorylation, culminating on cytoskeleton rearrangement and later pre-osteoblast adhesion.

33x37mm (600 x 600 DPI)